Polym. Bull. (2009) 62:487–502
DOI 10.1007/s00289-008-0029-4

ORIGINAL PAPER

Thermal response of low molecular weight poly-(*N*-isopropylacrylamide) polymers in aqueous solution

Ramón Pamies · Kaizheng Zhu · Anna-Lena Kjøniksen · Bo Nyström

Received: 27 October 2008 / Revised: 5 December 2008 / Accepted: 7 December 2008 /
Published online: 17 December 2008

Abstract Temperature-induced phase transition of three low-molecular-weight samples ($M_w < 1.2 \times 10^4$) of poly(*N*-isopropylacrylamide) was studied with the aid of turbidimetry, dynamic light scattering, and rheology. We have demonstrated that the lower critical solution temperature depends on the length of the chain and the concentration of the polymer in the low molecular weight range. The turbidity results show a transition peak in the turbidity curve at intermediate temperatures. This peak, as well as the cloud point, is shifted toward lower temperatures when the molecular weight and the concentration of the polymer increase. The DLS measurements disclose a fast and a slow relaxation mode, which in both cases are found to be diffusive. The fast mode is linked to the diffusion of small species in the solution, and the slow mode is associated with the formation of large aggregates. The formation of these aggregates is less pronounced in solutions of polymers with low molecular weight and the incipient aggregation is shifted to higher temperatures. The shear viscosity measurements show the formation of weak aggregates, which are easily broken in solutions of short polymers. This effect is less pronounced when the molecular weight of the sample is increased. At certain shear rates, temperature-induced transition peaks of the viscosity are observed.

Keywords PNIPAAM · Phase separation · Thermoresponsive polymers · Light scattering · Shear rate dependence

Introduction

Poly(*N*-isopropylacrylamide) (PNIPAAM) is a thermal responsive polymer that exhibits an intriguing heat-induced phase separation phenomenon in aqueous

R. Pamies · K. Zhu · A.-L. Kjøniksen · B. Nyström (✉)
Department of Chemistry, University of Oslo, P. O. Box 1033, Blindern, 0315 Oslo, Norway
e-mail: bo.nystrom@kjemi.uio.no

solution [1, 2] that has attracted both theoretical and technological interest [3–9] over the years. The debate in the literature has focused on whether hydrophobic interactions [10, 11], hydrogen-bonding effects [12, 13], or both [14, 15] are vital for this phase transition of PNIPAAM in aqueous solution. Since the hydrophobic effect is caused by changes in hydrogen bond interactions, these effects have been argued to be dependent of each other [16]. The lower critical solution temperature (LCST) of solutions of PNIPAAM has been reported to be in the range of 30–35 °C [16], but in the literature the LCST of PNIPAAM is frequently assigned to a value of 32 °C.

The initial investigations of aqueous solutions of PNIPAAM [1, 2] focused mainly on the temperature-induced coil-to-globule transition of the polymer without paying any attention on the impact of possible molecular weight and polydispersity effects. Later, several papers dealing with PNIPAAMs of high molecular weight and with narrow molecular weight distributions appeared. The coil-to-globule transition [12, 17] was established in very dilute aqueous solutions of high molecular weight PNIPAAM [18]. Fujishige et al. [19] reported that neither concentration nor molecular weight played a significant role in the phase transition of PNIPAAM homopolymer chains. However, the lowest value of the considered molecular weights was 5×10^4 and the concentration effect was evaluated only in the case of the highest molecular weight (8.4×10^6). There is a severe lack of investigations [20] addressing the effects of molecular weight and polymer concentration on the LCST or on the cloud point (CP).

Recently, the self-assembly of amphiphilic copolymers containing PNIPAAM has attracted a great deal of interest in the scientific community [21, 22], because of their potential applications in nanotechnology, reusable elastomeric materials, electronics, and drug delivery. These copolymers have often a fairly low molecular weight [23, 24] and the PNIPAAM block is short. For example, in previous papers [25–27] we have studied diblock and triblock copolymers with a typical PNIPAAM block with less than 120 monomers. It was shown that in aqueous solution the temperature at which these polymers formed large aggregates was strongly dependent upon the polymer concentration. In the light of this finding, the question arises whether the heat-induced phase separation of these copolymers is interrelated to the behavior of short PNIPAAM homopolymers in aqueous solution. The principal aim of this work is to examine the power of molecular weight and polymer concentration on the phase transition behavior of low-molecular weight samples of PNIPAAM. In addition, the heat-induced aggregation of PNIPAAM is characterized by dynamic light scattering (DLS) at the quiescent state, and the influence of shear flow on the aggregation process is a novel feature that is analyzed.

Experimental

Materials and synthesis of the polymers

All the chemicals used for the synthesis of the polymers were purchased from Aldrich and Fluka. *N*, *N*, *N*′, *N*″, *N*‴, *N*‴-(hexamethyl triethylene tetramine)

(Me_6TREN) was prepared according to a procedure described elsewhere [28]. *N*-isopropylacrylamide (NIPAAM) (Acros Organics) was recrystallized from toluene/hexane and dried under vacuum prior to use. Ethyl 2-chloropropionate (ECP) was distilled under reduced pressure and degassed before use. Copper(I) chloride from Aldrich was washed with glacial acetic acid, followed by washing with methanol and ethyl ether to remove impurities, and then dried under vacuum and kept under N_2 atmosphere. *N*,*N*′-dimethylformamide (DMF) was distilled under vacuum prior to use.

All water used in this study was purified with a Millipore Milli-Q system. The PNIPAAM samples were synthesized by means of atom transfer radical polymerization (ATRP) [29, 30], which was carried out in a water/DMF 50:50 (v/v) solvent mixture at 25 °C via an ATRP system with ECP/CuCl/Me_6TREN as the initiator/catalyst system (Scheme 1). The preparation and purification of these polymers were conducted under similar conditions as described previously [26, 31]. In a general procedure, NIPAAM (50 mmol, 5.66 g) was dissolved in 25 mL of a water/DMF 50:50 (v/v) solvent mixture [(NIPAAM) = 2.0 M] in a 50 mL Schlenk flask under magnetic stirring. The mixture was degassed by bubbling with argon for at least 1 h, before it was immersed in a water-bath that was kept at about 25 °C. A volume of 2 mL of the freshly prepared Cu(I)-Me_6TREN water stock solution (prepared by adding degassed water (7 mL) to CuCl (4 mmol, 0.396 g) and Me_6TREN (4 mmol, 1.1 mL) exposed to vigorous stirring under the influence of argon flow) was withdrawn via a syringe and quickly added to the above mixture. Degassed ECP (1 mmol, 128 μL) was then added via a Hamilton syringe and the polymerization reaction was then initiated. When the NIPAAM monomer conversion reached approximately 95% (after approximately 1 h, ^{1}H NMR analysis indicated that more than 95% of the NIPAAM had been polymerized (disappearance of the vinyl signals at $\delta = 5.5$–6.0 ppm), the polymerization was stopped by exposing the mixture to air and distilled water. The polymer was further purified by dialyzing against distilled water for several days using a dialysis membrane of regenerated cellulose with a

Scheme 1 Schematic illustration of the synthesis of PNIPAAM via ATRP

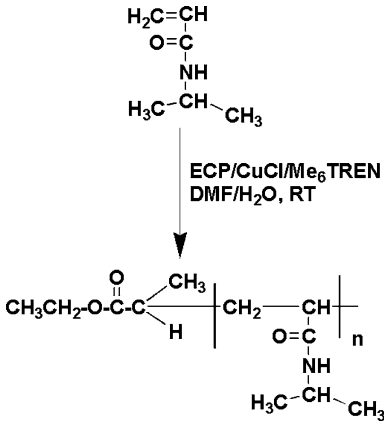

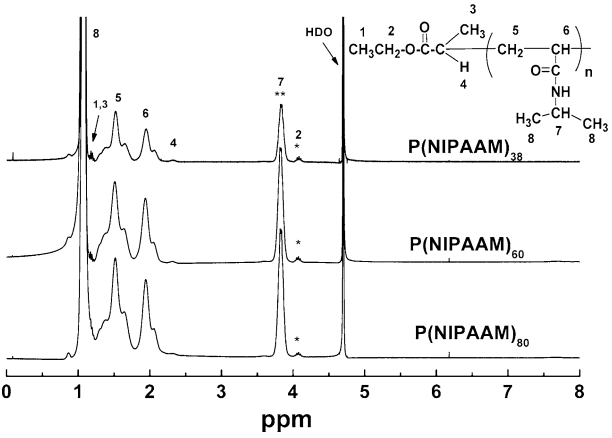

Fig. 1 ^{1}H NMR spectra of the synthesized polymers in D_2O (300 MHz)

molecular-weight-cutoff of 3,500. The white solid product was finally isolated by lyophilization.

The chemical compositions and structures of the synthesized homopolymers were all ascertained by ^{1}H NMR with a Bruker AVANCE DPX 300 NMR spectrometer, operating at 300.13 MHz at 25 °C by utilizing heavy water as the solvent. The repeating number of the NIPAAM units in all the polymers were basically calculated from the integral values of the characteristic peak (**7** in Fig. 1) of NIPAAM ($\delta = 3.82$ ppm, –C***H***$(CH_3)_2$, I_a) and the typical peak of the end group of ethyloxyl (**2** in Fig. 1) ($\delta = 4.08$ ppm ($CH_3C\boldsymbol{H}_2$O-), I_b) based on a simple equation: $n_{(NIPAAM)} = 2\,(I_a/I_b)$. We have successfully synthesized three PNIPAAM with different repeated units of NIPAAM ($n = 38$, $n = 60$ and $n = 80$) by simply adjusting the molar ratio of NIPAAM with the initiator ECP. The monomer/initiator (NIPAAM/ECP) ratios are 50/1, 80/1, and 100/1 for the samples with $n = 38$, $n = 60$, and $n = 80$, respectively.

The weight-average (M_w) and number-average (M_n) molecular weights and the polydispersity indexes (M_w/M_n) of the PNIPAAM samples were determined in very dilute aqueous solutions by means of asymmetric flow field-flow fractionation (AFFFF) methods [26, 32], and the results and data from the measurements are collected in Fig. 2. The experimental procedure and parameters are the same as reported previously [26]. It can be noted that all polymer samples have low molecular weights and narrow molecular weight distributions. From AFFFF data, we have recalculated the number of monomers, n, finding $n = 47$, 71, and 106 and we label the corresponding polymers as $P(NIPAAM)_{47}$, $P(NIPAAM)_{71}$ and $P(NIPAAM)_{106}$. The molecular weight data from AFFFF have been utilized because they are more accurate than the corresponding ones from ^{1}H NMR.

All samples were prepared by weighing the components and the solutions were homogenized by stirring for 1 day at ambient temperature.

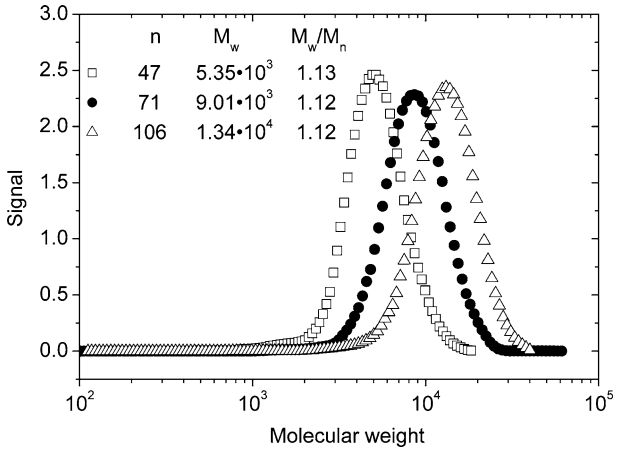

Fig. 2 Molecular weight distribution curves of the three P(NIPAAM)$_n$ samples in dilute aqueous solutions (0.01 M NaCl) with the aid of AFFFF. The inset shows the values of n, M_w, and M_w/M_n

Instrumentation

Turbidimetry

The temperature dependences of the turbidity of the copolymer solutions were monitored at a heating rate of 0.2 °C/min by employing an NK60-CPA cloud point analyzer from Phase technology, Richmond, BC, Canada. A detailed description of the apparatus and determination of turbidities have been given elsewhere [33]. This apparatus makes use of a scanning diffusive technique to characterize phase changes of the samples with high sensitivity and accuracy. The light beam from an AIGaAS light source, operating at 654 nm, was focused on the solution that was placed onto a specially designed glass plate that is coated with a thin metallic layer of very high reflectivity. Directly above the applied sample, an optical arrangement with a light scattering detector that continuously monitors the scattered intensity signal (S) from the measured solutions as it is subjected to prescribed temperature alterations. A direct empiric relationship between the signal and the turbidity (τ) is found [33] to be $\tau = 9.0 \times 10^{-9}\ S^{3.751}$. All the data from the cloud point analyzer will be presented in terms of turbidity.

Dynamic light scattering

The DLS experiments were conducted with the aid of an ALV/CGS-8F multi-detector compact goniometer system, with eight off fiber-optical detection units, from ALV-GmbH, Langen, Germany. The beam from an Uniphase cylindrical 22 mW He-Ne-laser, operating at a wavelength of 632.8 nm with vertically polarized light, was focused on the sample cell (10-mm NMR tubes) through a temperature-controlled cylindrical quartz container (with two plane-parallel windows), vat (the temperature constancy being controlled to within ± 0.01 °C

with a heating/cooling circulator), which is filled with a refractive index matching liquid (*cis*-decalin). Depending on the polymer concentrations, the polymer solutions were filtered through 5 or 0.8 μm filters (Millipore) directly into precleaned NMR tubes. The measurements were carried out under the influence of the same heating rate (0.2 °C/min) as for the turbidity experiments.

In the DLS measurements, the intensity correlation function was measured at eight scattering angles simultaneously in the range 22–141° with four ALV5000/E multiple-τ digital correlators. In the dilute concentration regime probed in this study, the scattered field obeys Gaussian statistics and the measured correlation function $g^2(q,\ t)$, where $q = (4\pi n/\lambda)\sin(\theta/2)$, with λ, θ, and n being the wavelength of the incident light in a vacuum, the scattering angle, and the refractive index of the medium, respectively, can be related to the theoretically amenable first-order electric field correlation function $g^1(q,\ t)$ by the Siegert relationship [34] $g^2(q,\ t) = 1 + B|g^1(q,\ t)|^2$, where B is usually treated as an empirical factor.

The correlation functions can be described by the sum of a single exponential and a stretched exponential

$$g^1(t) = A_\mathrm{f}\exp[-t/\tau_\mathrm{f}] + A_\mathrm{s}\exp\left[-(t/\tau_\mathrm{se})^\beta\right] \tag{1}$$

with $A_\mathrm{f} + A_\mathrm{s} = 1$. The parameters A_f and A_s are the amplitudes for the fast and the slow relaxation time, respectively. The variables τ_f and τ_se are the relaxation times characterizing the fast and the slow relaxation process, respectively. This type of bimodal relaxation process has been reported [33, 35, 36] from DLS studies on aggregating polymer systems of various natures. In the analysis of the correlation functions by means of Eq. 1, a nonlinear fitting algorithm was employed to obtain best-fit values of the parameters A_f, τ_f, τ_se and β appearing on the right-hand side of Eq. 1.

The fast mode is diffusive (q^2-dependent) for all the samples and it yields the mutual diffusion coefficient D ($\tau_\mathrm{f}^{-1} = Dq^2$) of molecularly dispersed species and small aggregates. The slow mode (the second term on the right-hand side of Eq. 1) characterizes the dynamics of large aggregates and this mode is also found to be diffusive.

The parameter τ_se in Eq. 1 is some effective relaxation time, and β ($0 < \beta \leq 1$) is a measure of the width of the distribution of relaxation times. The mean relaxation time for the slow mode is given by

$$\tau_\mathrm{s} = \frac{\tau_\mathrm{se}}{\beta}\Gamma\left(\frac{1}{\beta}\right) \tag{2}$$

where Γ is the gamma function. Depending on the stage of aggregation, the values of β are in the interval 0.7–0.95 in this study. Since both the relaxation modes are found to be diffusive, this enable us to calculate the apparent hydrodynamic radii ($R_\mathrm{h,f}$, and $R_\mathrm{h,s}$) from the fast and slow relaxation times, respectively, via the Stokes–Einstein relationship $D = k_B T/6\pi\eta R_\mathrm{h}$, where k_B is the Boltzmann constant, T is the absolute temperature, η is the solvent viscosity, and D is the diffusion coefficient of the different species in the solution.

Shear viscosity

A Paar-Physica MCR 300 rheometer, equipped with a cone-and-plate geometry with a cone angle of 1° and diameter of 75 mm, was utilized to monitor the shear viscosity of the polymer solutions. Even on dilute solutions, the rheometer operates effectively with this geometry, and the viscosity of water can readily be determined over an extended shear-rate domain. The solutions were introduced onto the plate and to prevent evaporation of water, the free surface of the sample was always covered with a thin layer of low-viscosity silicone oil that virtually did not affect the solution viscosity. The instrument is equipped with a temperature unit (Peltier plate) that provides a fast and accurate alteration of the temperature over the studied temperature range. The temperature control is better than $\pm$ 0.05 °C over the considered temperature domain. The measurements were conducted at a constant shear rate with a temperature gradient of 0.2 °C/min, as in the turbidity and DLS experiments.

Results and discussion

By using turbidimetry, DLS, and shear viscosity, this work demonstrates that the value of the LCST for aqueous solutions of PNIPAAM is dependent on both the length of the chain and the polymer concentration. These effects should be taken into account in the design of temperature responsive copolymers containing a NIPAAM block.

Turbidimetry

Figure 3 shows turbidity results for the three PNIPAAM samples at a constant value of the concentration of 1 wt%. When the temperature rises, PNIPAAM chains become more hydrophobic and intermolecular interactions occur, resulting in the formation of larger aggregates that leads to an increment in the turbidity values at a certain temperature, known as CP. The CPs are determined as the temperature where an incipient increase in the turbidity is observed (see lower inset in Fig. 3). For all molecular weights, the turbidity exhibits a steep transition as the temperature rises and at higher temperatures the turbidity passes through a maximum. After the maximum, the density of hydrophobic segments in the core is high, and the close packing of these segments in the core results in contraction of the clusters. The hydrophobic interactions are more intensive as the polymer chain becomes longer, and the incipient aggregation takes place at lower temperatures. We notice from the upper inset in Fig. 3 that the value of the cloud point decreases with increasing molecular weight of the polymer. This clearly demonstrates that the length of the chain is a crucial variable that affects the phase transition of PNIPAAM homopolymers in the molecular weight range studied in this work. In dilute aqueous solutions of an amphiphilic polymer like PNIPAAM of fairly short polymer chains, the number of hydrophobic segments in the chain will rise with increasing molecular weight of PNIPAAM and the collision frequency and the sticking

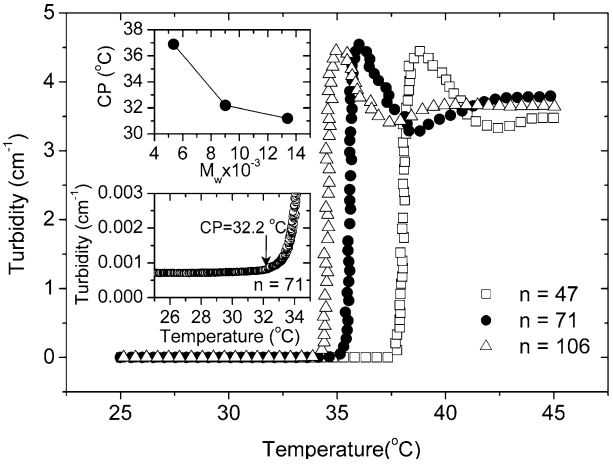

Fig. 3 Temperature dependences of the turbidity during a heating rate of 0.2 °C/min for P(NIPAAM)$_n$ at a constant concentration of 1 wt%. The upper inset shows the effect of molecular weight on the cloud point. The lower inset shows how the CP is determined from the incipient increase of the turbidity

probability are enhanced. This leads to the formation of aggregates at a lower temperature and a depression of the cloud point. However, at high molecular weights of PNIPAAM this effect is lost, because the number of hydrophobic segments plays a less dominate role for long polymer chains [19]. This is probably the reason why the impact of molecular weight on CP for aqueous solutions of PNIPAAM has not been disclosed earlier.

Effects of both the length of the polymer and polymer concentration on the temperature dependence of the turbidity are depicted in Fig. 4a–c. The general picture that emerges is that both longer polymer chains and higher concentration depress the value of CP and the transition zone seems to be more distinct at higher molecular weight. The results clearly reveal that the value of the cloud point is strongly affected by molecular weight and concentration (see Fig. 4d). However, at higher polymer concentration the effect of molecular weight on CP disappears because when the semidilute concentration regime is approached, the molecular species overlap each other and the individual features of the molecules vanish. This situation is reminiscent of the behavior for polymer solutions, when they are transformed from the dilute to the semidilute regime, where the polymer chains form a transient network and the molecules individuality is lost. We notice that the concentration dependence of CP is less pronounced as the molecular weight of the sample is increased; this feature is consistent with the idea discussed above that the influence of molecular weight on the value of CP diminishes at sufficiently high molecular weights.

The influence of temperature and polymer concentration on CP can be rationalized in the following scenario. As the temperature rises, the polymer molecules become more “sticky” (the hydrophobicity increases) and when they collide aggregates are formed, giving rise to enhanced turbidity. The depression of CP with increasing polymer concentration may be interpreted with resort to the

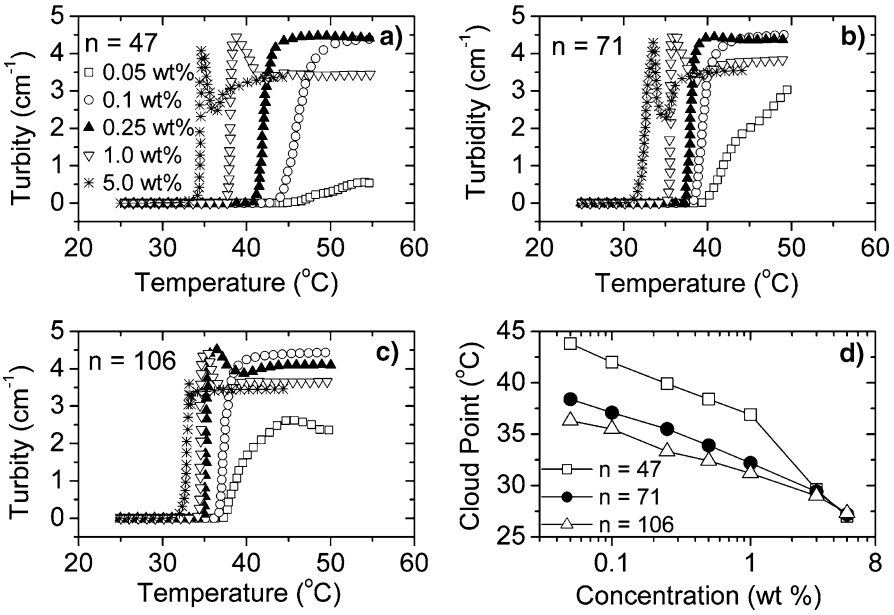

Fig. 4 **a–c** Effects of concentration and molecular weight on the turbidity for the P(NIPAAM)$_n$ samples and concentrations indicated. **d** The concentration dependences of the cloud point for the polymers indicated

effective Flory-Huggins interaction parameter χ_{eff} [37, 38], where χ_{eff} is a function of both temperature (T) and concentration (c), i.e., $\chi_{eff} = \chi_{eff}(T, c)$. At a given temperature, the raise of χ_{eff} with increasing polymer concentration is ascribed to poorer solvent conditions, or in the case of associating polymer solutions to stronger association. The effects of polymer concentration and temperature on the formation of aggregates in polymer solutions have been addressed in several theoretical studies [39–45]. De Gennes elaborated a model [41] for the interpretation of the association behavior in aqueous poly(ethylene oxide) solutions. In this model, the concentration dependence of χ_{eff} is ascribed to attractive interactions leading to stable clusters of $n > 2$ monomers (e.g., micelles) while binary monomer-monomer interactions remain repulsive. This is a type of two-state model for associating polymers, where a dynamic equilibrium between "clustered" and "non-clustered" monomers is considered. This model predicts a situation at very poor thermodynamic conditions, where a very dilute solution of individual polymer species coexists with a dense polymer phase (i.e., aggregates). A scenario emerges where increasing the polymer concentration reduces solvent quality, e.g., a solution of a polymer in water at room temperature exhibits good solvent features at low polymer concentration and poor solvent properties at high concentration. In a general approach developed by Painter et al. [43] for polymer solutions, the concentration dependence of χ_{eff} is attributed to the interplay between intrachain and interchain contacts. In the framework of these models, the observed decrease of CP with rising

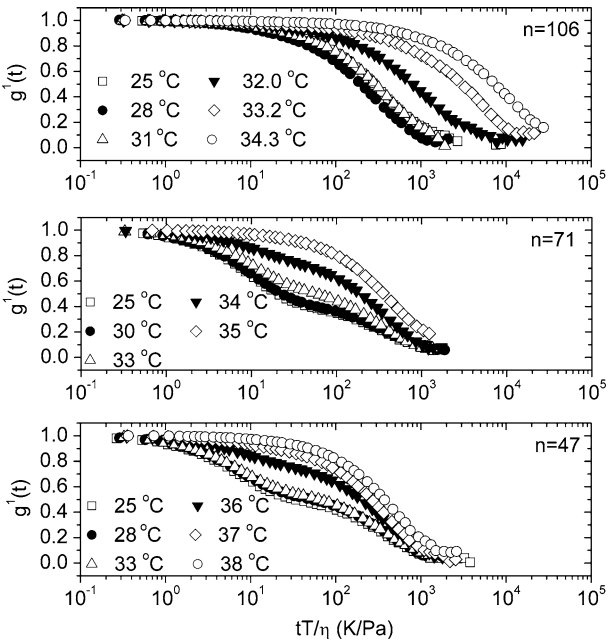

Fig. 5 First-order field correlation function (at a scattering angle of 90°; every second data point is shown) versus the quantity tT/η for 1 wt% solutions of P(NIPAAM)$_n$ with indicated values of n

polymer concentration can be attributed to more intense intermolecular association at higher concentration, leading to a reduction of the cloud point temperature.

Dynamic light scattering

The normalized correlation functions at a scattering angle of 90° for 1 wt% solutions of P(NIPAAM)$_n$ were recorded continuously at a heating rate of 0.2 °C/min (the same rate as before) and they are displayed in Fig. 5 in the form of semilogarithmic plots. Each measurement took 1 min and the temperature refers to the mean temperature during an experiment. To take into account trivial changes of the solvent viscosity with temperature, the correlation function data have been plotted against the quantity tT/η. For the solutions of P(NIPAAM)$_{47}$ and P(NIPAAM)$_{71}$ the decays of the correlation functions can initially be described by a single exponential, followed at longer times by a stretched exponential (Eq. 1). As can be seen from the inset plot in Fig. 6, the value of the amplitude of the fast mode (A_f) decreases markedly with raising temperature for both polymer fractions. This is because the size and number of the formed aggregates increase and the impact of small entities on the decay of the correlation function is strongly reduced. At this stage, the values of A_f is very low and it is not possible to extract the fast relaxation mode, so we describe the decay of the correlation function by means of a single stretched exponential.

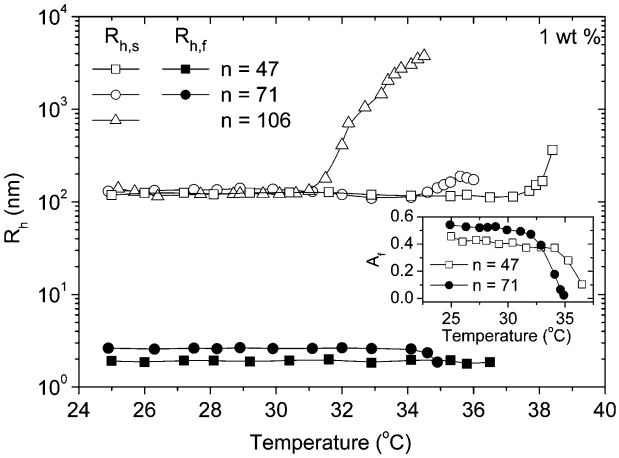

Fig. 6 Temperature dependencies of the apparent hydrodynamic radii determined from the fast relaxation time ($R_{h,f}$) and the slow relaxation time (R) through the Stokes–Einstein relation for 1 wt% solutions of P(NIPAAM)$_n$. The inset plot shows the temperature influence on the amplitude of the fast mode A_f

For the P(NIPAAM)$_{106}$ solutions, it is not feasible to extract the fast single exponential decay at any temperature owing to the large aggregates that are formed even at room temperature. Therefore, the decays of these correlation functions have been portrayed with the aid of a single stretched exponential. At all conditions, the relaxation modes are diffusive. The general feature in Fig. 5 is that the tail of the correlation function is shifted toward longer times as the temperature increases, which announces the temperature-induced growth of association complexes.

Figure 6 shows the temperature dependences of the hydrodynamic radii, corresponding to the fast mode ($R_{h,f}$) and the slow mode ($R_{h,s}$) for 1 wt% solutions of P(NIPAAM)$_n$ with $n = 47$, 71, and 106. The values of $R_{h,f}$ are 2 nm for P(NIPAAM)$_{47}$ and 3 nm for P(NIPAAM)$_{71}$, which reflects the size of single molecules and/or small aggregates. This seems to support the conjecture of de Gennes [41] about the dynamical equilibrium and coexistence of molecularly dispersed molecules and aggregates. At high temperatures, an incipient compression of the species is detected for the solution of P(NIPAAM)$_{71}$ at the onset of interchain association. This type of behavior has been reported [32, 46, 47] for copolymers of various natures. This contraction is not observed for the solution of the PNIPAAM with the shortest chains ($n = 47$), probably due to the lower flexibility of the chains.

The temperature dependence of $R_{h,s}$, extracted from the slow mode, displays a different pattern of behavior for the population of the large clusters portrayed by this mode. At low temperatures (weak hydrophobic interactions), there is no significant difference in the size of the clusters because at low temperatures the aggregation number is almost the same for the three samples, and since the molecular weight of the PNIPAAM fractions is not very different (the size of the molecularly dispersed molecules is not very different for the three samples) the clusters in the solutions should be of almost the same size. The temperature-induced growth of the

Table 1 Values of CP from turbidimetry and values estimated from $R_{h,s}$ data for 1 wt% solutions of P(NIPAAM)$_n$

See text for details

n	From the deviation of $R_{h,s}$ (°C)	From turbidimetry CP (°C)	Deviation (%)
47	37.2	36.9	0.8
71	34.1	32.2	5.6
106	31.0	31.2	0.6

aggregates commences at a lower temperature with increasing molecular weight of the sample. This is compatible with the trend observed from the turbidity measurements, and this demonstrates that in dilute solutions the molecular weight plays an important role for the phase transition behavior.

It is interesting to note that the temperatures determined from the incipient deviation of $R_{h,s}$ from the baseline of the data at elevated temperatures are fairly close to the values of CP estimated from the turbidity measurements (see Table 1). This indicates that the growth of the clusters is a harbinger of phase transition behavior.

Shear viscosity

The temperature-induced association behavior of solutions of PNIPAAM, probed by turbidimetry and DLS, has revealed the formation of large complexes at elevated temperatures under quiescent conditions. The growth of these aggregates is related to the stability of these clusters. To gain insight into this matter, we have examined the effect of shear flow on the aggregation process. Figure 7 shows the influence of shear rate on the relative viscosity, η_{rel} ($\eta_{rel} \equiv \eta/\eta_{water}$, with η_{water} the solvent viscosity at a given temperature) for 1 wt% solutions of P(NIPAAM)$_n$ ($n = 47$, 71 and 106) with the same heating rate as that used in DLS and turbidimetry. In the solution of P(NIPAAM)$_{47}$, a strong upturn of the relative viscosity is registered at the lowest shear rate (10 s^{-1}) for temperatures above 40 °C, whereas at higher shear rates almost no effect of temperature on η_{rel} is found. This suggests that association structures are formed at a low shear rate, whereas higher shear rates suppress the buildup of aggregates. It should be noted that the aggregate growth temperature for the viscosity is appreciably higher than that obtained from the DLS data at the quiescent state (cf. Fig. 6). This indicates that the shear flow reduces the rate of growth of aggregates.

It is well known that in systems of sticky species, shear flow bring polymer molecules close to each other, faster than Brownian motion, and the formation of aggregates can be accelerated [48]. This is called orthokinetic aggregation and usually arises at low shear rates. At high shear rates, the growth rate of aggregates is often depressed or even arrested, and giant clusters are disrupted under the influence of strong shear stresses [49–51]. In a recent study [52] on aqueous solutions of a high molecular weight PNIPAAM sample, a viscosity maximum was observed just before the demixing temperature and the viscosity decreases strongly when the two phase region is approached. The maximum was ascribed to network formation, whereas the maximum in this work is attributed to evolution of aggregates. The network was disrupted at higher shear rates.

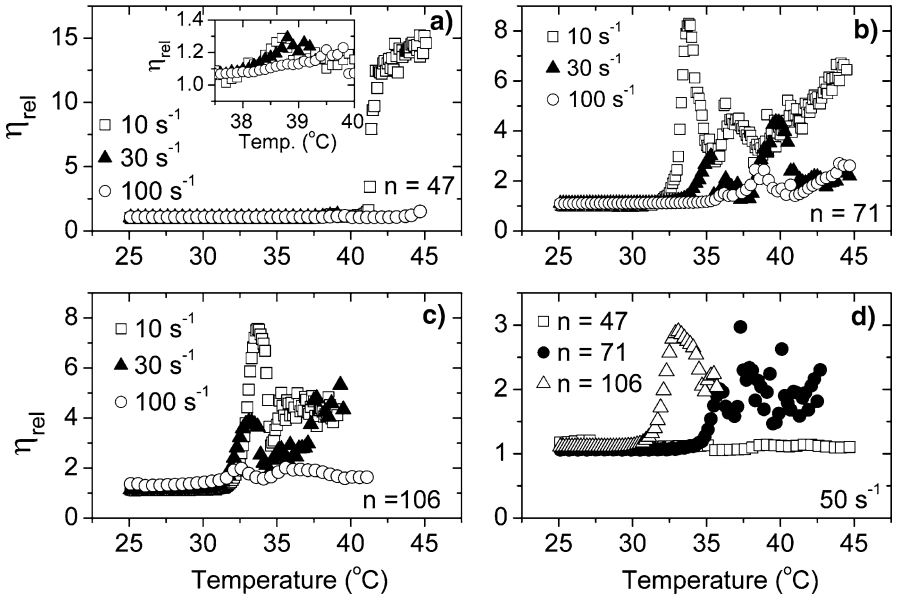

Fig. 7 **a–c** Effects of temperature and shear rate on the relative viscosity for 1 wt% solutions of P(NIPAAM)$_n$ with the indicated values of n. The inset is an amplification of the data before the transition zone. **d** A comparison of the viscosity data for 1 wt% solutions of the different PNIPAAM fractions at a constant value (50 s^{-1}) of the shear rate

When the solutions of P(NIPAAM)$_{71}$ and P(NIPAAM)$_{106}$ are exposed to shear stresses a different picture emerges. In this case, narrow transition peaks appear at low shear rates for both samples. This feature suggests that the formation of large complexes is favored in the earlier stage of the association process, but when the aggregates are sufficiently huge the structures breakup under the influence of shear flow. The reason why viscosity peaks are developed for the two higher molecular weight PNIPAAM fractions but not for P(NIPAAM)$_{47}$ is probably that stronger association complexes are formed in these cases because of the higher intensity of the hydrophobic interactions. At high shear rate, no transition peak is evolved since the growth of large aggregates is repressed.

A comparison of the effect of temperature on the relative viscosity for 1 wt% solutions of the studied PNIPAAM fractions at a fixed shear rate of 50 s^{-1} is depicted in Fig. 7d. For the solution of the lowest molecular weight (P(NIPAAM)$_{47}$), the relative viscosity is virtually unaffected by temperature in the considered temperature domain. For the solutions of P(NIPAAM)$_{71}$ and P(NIPAAM)$_{106}$, transition peaks appear but the peak is located at a lower temperature and more pronounced for the solution with the polymer of the highest molecular weight. This difference in behavior between the samples can directly be traced to the augmented intensity of the hydrophobic interactions for the polymer with the longest polymer chains and the highest number of hydrophobic segments.

Conclusions

The results from this work have clearly demonstrated that the value of the cloud point for aqueous solutions of rather monodisperse low molecular weight poly(*N*-isopropylacrylamide) samples is considerably affected by both the molecular weight and the polymer concentration. Longer polymer chains and higher concentration, both depress the value of the cloud point. At polymer concentrations approaching the semidilute regime, the molecular weight dependence of the CP gradually disappears.

The DLS results divulge two populations of species—molecularly dispersed entities and association structures. The temperature-growth of the aggregates is portrayed by the slow mode, and the transition starts at a lower temperature with increasing molecular weight of the polymer and it becomes more prominent for the longer polymer chains. The temperatures for the onset of the growth of the aggregates for the different molecular weights are fairly close to the corresponding values of CP determined from the turbidity measurements.

The shear viscosity experiments show that for the PNIPAAM sample with the lowest molecular weight, the tendency of forming aggregates at elevated temperatures is suppressed at all the shear rates, except at the lowest shear rate where large association complexes are developed at high temperatures. For the solutions of the higher two molecular weights, marked transition peaks are evolved at moderate shear rates and virtually no association complexes are formed at high shear rates. These findings can be rationalized in terms of more intensive hydrophobic interactions at elevated temperatures for the longer polymer chains that are more hydrophobic. The results from this work can provide vital information in the design of new thermoresponsive block copolymers that can be modulated to self-assembly at specific temperatures.

Acknowledgments We gratefully acknowledge support from the Norwegian Research Council (177665/V30). R. P. acknowledges a postdoctoral fellowship from Fundación Séneca-CARM.

References

1. Scarpa JS, Mueller DD, Klotz IM (1967) Slow hydrogen-deuterium exchange in a non-α-helical polyamide. J Am Chem Soc 89:6024–6030
2. Heskins M, Gillet JE (1968) Solution properties of poly(N-isopropylacrylamide). J Macromol Sci Chem A2:1441–1455
3. Guillet JE, Heskins M, Murray DG (1985) Polymeric flocculants. US patent 4, 536,294
4. Dong LC, Yan Q, Hoffman AS (1992) A novel-approach for preparation of pH-sensitive hydrogels for enteric drug delivery. J Control Release 19:141–152
5. Hayashi H, Kono K, Takagishi T (1996) Temperature-controlled release property of phospholipid vesicles bearing a thermo-sensitive polymer. Biochim Biophys Acta 1280:127–134
6. Deng Y, Xiao H, Pelton R (1996) Temperature-sensitive flocculants based on poly(N-isopropylacrylamide-co-diallyldimethylammoniumchloride). J Colloid Interface Sci 179:188–193
7. Hirotsu S, Hirokawa Y, Tanaka T (1987) Volume-phase transitions of ionized N-isopropylacrylamide gels. J Chem Phys 87:1392–1395
8. Beltran S, Baker JP, Hooper HH, Blanch HW, Prausnitz JM (1991) Swelling equilibria for weakly ionizable, temperature-sensitive hydrogels. Macromolecules 24:549–551

9. Ringsdorf H, Sackmann E, Simon J, Winnik FM (1993) Interactions of liposomes and hydrophobically-modified poly-(N-isopropylacrylamides)—an attempt to model the cytoskeleton. Biochim Biophys Acta 1153:335–344
10. Kubota K, Fujishige S, Ando I (1990) Single-chain transition of poly(N-isopropylacrylamide) in water. J Phys Chem 94:5154–5158
11. Kubota K, Fujishige S, Ando I (1990) Solution properties of poly(N-isopropylacrylamide) in water. Pol J 22:15–20
12. Matsuyama A, Tanaka T (1991) Theory of solvation-induced reentrant coil globule transition of an isolated polymer-chain. J Chem Phys 94:781–786
13. Prange MM, Hooper HH, Prausnitz JM (1989) Thermodynamics of aqueous systems containing hydrophilic polymers or gels. AIChE J 35:803–813
14. Winnik FM (1990) Phase transition of aqueous poly-(N-isopropylacrylamide) solutions: a study by non-radiative energy transfer. Polymer 31:2125–2134
15. Schild HG, Tirrel DA (1991) Cononsolvency in mixed aqueous-solution of poly(N-isopropylacrylamide). Macromolecules 24:948–952
16. Schild HG (1992) Poly(N-isopropylacrylamide)—experiment, theory and application. Prog Polym Sci 17:163–249
17. Meewes M, Ricka J, de Silva M, Nyffenegger R, Binkert Th (1991) Coil globule transition of poly(N-isopropylacrylamide)—a study of surfactant effects by light-scattering. Macromolecules 24:5811–5816
18. Wu C, Zhou S (1995) Laser light scattering study of the phase transition of poly(N-isopropylacrylamide) in water. 1. Singe chain. Macromolecules 28:8381–8387
19. Fujishige S, Kubota K, Ando I (1989) Phase-transition of aqueous-solutions of poly(N-isopropylmethacrylamide) and poly(N-isopropylmethacrylamide). J Phys Chem 93:3311–3313
20. Badiger MV, Rajamohanan PR, Kulkarni MG, Ganapathy S, Mashelkar RA (1991) Proton MASS-NMR: a new tool to study thermoreversible transition in hydrogels. Macromolecules 24:106–111
21. Lazzari M, Liu G, Lecommandoux S (2006) Block copolymers in nanoscience (eds) Wiley-VCH, Weinheim
22. Malmsten M (2002) Surfactants and polymers in drug delivery. Marcel Dekker, NY
23. Wei H, Cheng C, Chang C, Chen W-Q, Cheng S-X, Zhang X-Z, Zhuo R-X (2008) Synthesis and applications of shell cross-linked thermoresponsive hybrid micelles based on poly(N-isopropylacrylamide-co-3-(trimethoxysilyl)propyl methacrylate)-b-poly(methyl methacrylate). Langmuir 24:4564–4570
24. Ha DI, Lee SB, Chong MS, Lee YM, Kim SY, Park YH (2006) Preparation of thermo-responsive and injectable hydrogels based on hyaluronic acid and poly(N-isopropylacrylamide) and their drug release behaviors. Macromol Res 14:87–93
25. Kjøniksen A-L, Zhu K, Pamies R, Nyström B (2008) Temperature-induced formation and contraction of micelle-like aggregates in aqueous solutions of thermoresponsive short-chain copolymers. J Phys Chem B 112:3294–3299
26. Zhu K, Jin H, Kjøniksen A-L, Nyström B (2007) Anomalous transition in aqueous solutions of a thermoresponsive amphiphilic diblock copolymer. J Phys Chem B 111:10862–10870
27. Kjøniksen A-L, Zhu K, Karlsson G, Nyström B (2009) Novel transition behavior in aqueous solutions of a charged thermoresponsive triblock copolymer. Colloids Surf A 333:32–45
28. Ciampolini M, Nardi N (1966) Five-coordinated high-spin complexes of bivalent cobalt, nickel, and copper with Tris(2-dimethylaminoethyl)amine. Inorg Chem 5:41–44
29. Hawker CJ, Bosman AW, Harth E (2001) New polymer synthesis by nitroxide mediated living radical polymerizations. Chem Rev 101:3661–3688
30. Matyjaszewski K, Xia J (2001) Atom transfer radical polymerization. Chem Rev 101:2921–2990
31. Masci G, Giacomelli L, Crescenzi V (2004) Atom transfer radical polymerization of N-isopropylacrylamide. Macromol Rapid Commun 25:559–564
32. Modig G, Nilsson L, Bergenståhl B, Wahlund KG (2006) Homogenization-induced degradation of hydrophobically modified starch determined by asymmetrical flow field-flow fractionation and multi-angle light scattering. Food Hydrocoll 20:1087–1095
33. Kjøniksen AL, Laukkanen A, Galant C, Knudsen KD, Tenhu H, Nyström B (2005) Association in aqueous solutions of a thermo-responsive PVCL-g-$C_{11}EO_{42}$ copolymer. Macromolecules 38:948–960
34. Siegert AJF (1943) Massachusetts Institute of Technology, Radiation Lab Report No. 465

35. Kjøniksen A-L, Nyström B, Tenhu H (2003) Characterisation of thermally controlled chain association in aqueous solutions of poly(N-isopropylacrylamide)-g-poly(ethylene oxide). Dynamic light scattering. Colloids Surf A 228:75–83
36. Chen H, Ye X, Zhang G, Zhang Q (2006) Dynamics of thermoresponsive PNIPAM-g-PEO copolymer chains in semi-dilute solution. Polymer 47:8367–8373
37. Malcolm GN, Rowlinson JS (1957) The thermodynamics properties of aqueous solutions of polyethylene glycol, polypropylene glycol and dioxane. Trans Faraday Soc 53:921–931
38. Baulin VA, Halperin A (2002) Concentration dependence of the Flory (x) parameter within two-state models. Macromolecules 35:6432–6438
39. Karlström G (1985) A new model for upper and lower critical solution temperatures in poly(ethylene oxide) solutions. J Phys Chem 89:4962–4964
40. Matsuyama A, Tanaka F (1990) Theory of solvation-induced reentrant phase-separation in polymer-solutions. Phys Rev Lett 65:341–344
41. De Gennes P-G (1991) Model for the tack of molten polymers. CR Acad Sci Paris Ser II 313:1415–1418
42. Bekiranov S, Bruinsma R, Pincus P (1993) Solution behavior of polyethylene oxide in water as a function of temperature and pressure. Phys Rev E 55:577–585
43. Painter PC, Berg LP, Veytsman B, Coleman MM (1997) Intramolecular screening in nondilute polymer solutions. Macromolecules 30:7529–7535
44. Semenov AN, Rubinstein M (1998) Thermoreversible gelation in solutions of associative polymers. 1. Statics. Macromolecules 31:1373–1385
45. Borisov OV, Halperin A (1999) Polysoaps within the p-cluster model: solutions and brushes. Macromolecules 32:5097–5105
46. Lessard DG, Ousalem M, Zhu XX, Eisenberg A, Carreau PJJ (2003) Study of the phase transition of poly(N,N-diethylacrylamide) in water by rheology and dynamic light scattering. Polym Sci Part B Polym Phys 41:1627–1637
47. Chen H, Zhang Q, Li J, Ding Y, Zhang G, Wu C (2005) Formation of mesoglobular phase of PNIPAM-g-PEO copolymer with a high PEO content in dilute solutions. Macromolecules 38:8045–8050
48. Larson RG (1999) The structure and rheology of complex fluids. Oxford University Press, New York
49. Doi M, Chen D (1989) Simulation of aggregating colloids in shear flow. J Chem Phys 90:5271–5278
50. Brunet E, Degré G, Okkels F, Tabeling P (2005) Aggregation of paramagnetic particles in the presence of a hydrodynamic shear. J Colloid Interface Sci 282:58–68
51. Potanin AA (1991) On the mechanism of aggregation in the shear-flow of suspensions. J Colloid Interface Sci 145:140–157
52. Badiger MV, Wolf BA (2003) Shear induced demixing and rheological behavior of aqueous solutions of poly(N-isopropylacrylamide). Macromol Chem Phys 204:600–606